MOLECULAR AND CELLULAR BIOLOGY, Feb. 2006, p. 1549–1557 Vol. 26, No. 4
0270-7306/06/$08.00+0 doi:10.1128/MCB.26.4.1549–1557.2006

Sialoadhesin-Deficient Mice Exhibit Subtle Changes in B- and T-Cell Populations and Reduced Immunoglobulin M Levels

Cornelia Oetke,[1] Mary C. Vinson,[2] Claire Jones,[1] and Paul R. Crocker[1]*

The Wellcome Trust Biocentre, School of Life Sciences, University of Dundee, Dundee, United Kingdom,[1] and Neurology Centre of Excellence for Drug Discovery, GlaxoSmithKline, Essex, United Kingdom[2]

Received 25 August 2005/Returned for modification 23 October 2005/Accepted 30 November 2005

Sialoadhesin (Sn, also called Siglec-1 or CD169) is a transmembrane receptor and the prototypic member of the Siglec family of sialic acid binding immunoglobulin-like lectins. It is expressed on specialized subsets of resident macrophages in hematopoietic and lymphoid tissues and on inflammatory macrophages. In order to investigate its function, we generated Sn-deficient mice and confirmed that these mice are true nulls by fluorescence-activated cell sorter analysis and immunohistochemistry. Mice deficient in Sn were viable and fertile and showed no developmental abnormalities. Analysis of cell populations revealed no differences in bone marrow, peritoneal cavity, and thymus, but there was a small increase in CD8 T cells and a decrease in B220-positive cells in spleens and lymph nodes of Sn-deficient mice. Furthermore, in spleen there was a slight decrease in follicular B cells with an increase in numbers of marginal zone B cells. B- and T-cell maturation as well as responses to stimulation with thioglycolate were only slightly affected by Sn deficiency. Immunoglobulin titers in Sn-deficient mice were significantly decreased for immunoglobulin M (IgM) but similar for IgG subclasses. These results suggest a role for sialoadhesin in regulating cells of the immune system rather than in influencing steady-state hematopoiesis.

Sialoadhesin (Sn, also called CD169 or Siglec-1) was first described as a nonphagocytic sheep erythrocyte binding receptor (SER) of mouse macrophages (10) and later shown to be a prototypic member of the Siglec family of sialic acid binding immunoglobulin-like lectins (11). A total of 11 Siglecs in humans and 8 Siglecs in the mouse have been identified, with various tissue distributions and preferences for the type of sialic acid recognized and its linkage to the penultimate sugar (12). Siglecs consist of an N-terminal V-set domain that contains the sialic acid binding site followed by variable numbers of C2-set domains, a transmembrane domain, and a cytoplasmic tail. In contrast to several of the rapidly evolving CD33-related Siglecs, Sn has a well-defined ortholog in all of the mammalian species examined, including mouse, rat, pig, chimpanzee, and human (1, 16, 46). The amino acid identity varies from 69 to 78% between mouse, pig, and human, with the highest identity being found in the N-terminal V-set domain and the lowest in the intracellular region (1, 16, 46). Sn has an unusually large number, 16, of C2-set domains, a conserved feature that may be important for its ability to mediate cell-cell interactions (33). In contrast to most other Siglecs, Sn does not contain any inhibitory tyrosine-based motifs in its relatively short cytoplasmic tail (7).

The cellular expression pattern of Sn is well conserved between mammalian species, being restricted to subsets of tissue macrophages, especially those in secondary lymphoid organs (6, 16, 41). In the mouse, Sn is highly expressed on macrophages within the subcapsular sinus and medulla of lymph nodes and on marginal metallophilic macrophages in spleen (9, 26). Intermediate levels are expressed on 50 to 90% of resident bone marrow macrophages, and low but detectable levels are found for Kupffer cells, red pulp macrophages, and alveolar macrophages (9, 10). Besides expression on subsets of resident tissue macrophages, Sn is expressed at high levels on inflammatory macrophages in rheumatoid arthritis, atherosclerosis (16), experimental autoimmune uveoretinitis (17), experimental allergic encephalomyelitis (37), and nephritis (5) and on macrophages that infiltrate human breast tumors (35). Very recent reports show that Sn can also be expressed by certain dendric cells (2, 20) and on inflammatory blood monocytes following human immunodeficiency virus infection (39).

The biological functions of Sn are still unresolved, but its structural features and high conservation on macrophages point to a role in mediating cell-cell interactions. Cells from the granulocyte lineage have been shown to express high levels of Sn counter-receptors, and Sn was shown to cluster in contact zones between Sn-positive macrophages and developing granulocytes in bone marrow (8, 13). This gave rise to the hypothesis that Sn may be involved in granulocyte development or the retention of granulocytes within the bone marrow or at sites of inflammation. Other studies have demonstrated the binding of Sn to murine erythroleukemia cells (42) as well as T and B cells (44). In the spleen and lymph nodes, B cells are located adjacent to highly Sn-positive macrophages and, in a graft-versus-leukemia model, Sn-positive macrophages in the liver were seen to form clusters with CD8 T cells (32). It is therefore tempting to speculate that Sn may be involved in some aspects of lymphocyte trafficking or activation. The glycoproteins CD43, PSGL-1, and MUC1 have been shown to bind to Sn in a sialic acid-dependent manner and may therefore represent in vivo counter-receptors for Sn (35, 45). In addition, on its extracellular region, Sn displays up to 15 *N*-linked glycans which have been shown to function as carbohydrate ligands for other

* Corresponding author. Mailing address: The Wellcome Trust Biocentre, University of Dundee, Dow Street, Dundee DD1 5EH, United Kingdom. Phone: 44-1382-345781. Fax: 44-1382-345783. E-mail: p.r.crocker@dundee.ac.uk.

mammalian lectins, such as the cysteine-rich domain of the mannose receptor which binds GalNAc-4-SO_4-modified glycans (23, 25) and the macrophage galactose C-type lectin 1 (MGL-1) which recognizes Gal and GalNAc residues (21). In the latter case, Sn-MGL-1 interactions have been implicated in the trafficking functions of macrophages migrating from skin into draining lymph nodes during immune responses.

Although Sn does not mediate phagocytosis, there are some indications that it may be involved in endocytosis of smaller particles and certain pathogens. By immunoelectron microscopy, Sn was found in endosome-like membrane invaginations that were clearly distinct from phagosomes and lysosomes or Golgi (41). Sn on porcine alveolar macrophages has been shown to be the receptor for porcine reproductive and respiratory syndrome virus and to mediate the viral entry via endocytosis (46). In addition, Sn can bind the sialylated lipooligosaccharide of *Neisseria meningitidis* and enhance phagocytosis of intact bacteria by macrophages (18).

In the present study, we describe the generation of Sn-deficient mice in order to address the biological functions of Sn in vivo. We demonstrate that these mice are viable and show only a minimal phenotype under specific-pathogen-free conditions. Analysis of cell populations in bone marrow, blood, and peritoneal cavity did not reveal any major alteration, and we also did not observe any major differences in acute inflammatory responses to thioglycolate compared with wild-type controls. However, there were small differences in the CD8-positive T-cell population and in B220-positive B cells in spleen and lymph nodes. The immunoglobulin G (IgG) titers were normal, but there was a reduction in serum IgM in Sn-deficient mice. This overall minimal phenotype makes these mice a good model to investigate the role of Sn following immune responses and in inflammatory diseases like rheumatoid arthritis.

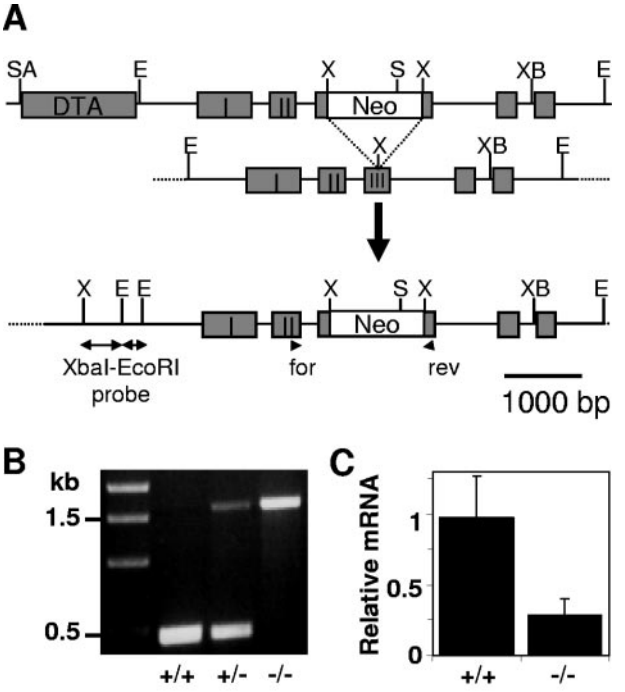

FIG. 1. Targeted disruption of the *Sn* gene. (A) The Sn-targeting construct contains a neomycin cassette (Neo) in the XhoI site of exon III with flanking 2.5-kb and 2.4-kb homology arms and a diphtheria toxin A (DTA) cassette for negative selection. The wild-type locus (middle) and targeted gene locus (bottom) are shown. Arrows indicate the XbaI-EcoRI probe used for Southern screening and the primers (for and rev) used for genotyping by PCR. Enzyme abbreviations are E, EcoRI; S, SphI; SA, SalI; X, XhoI; and XB, XbaI. (B) Representative example of PCR screens of DNA from wild-type, heterozygous mutant, and homozygous mutant mice. (C) Quantitative real-time PCR of Sn cDNA derived from total spleen RNA of wild-type and Sn-deficient mice. Data shown are means ± standard deviations (SD) of two independent experiments analyzing four mice each for both genotypes.

MATERIALS AND METHODS

Reagents and antibodies. Unless otherwise stated, all reagents were purchased from Sigma-Aldrich (Dorset, United Kingdom), including goat anti-human IgG Fc antibody (fluorescein isothiocyanate [FITC]) and goat anti-rabbit IgG (tetramethyl rhodamine isocyanate). Antibodies against CD1d (1B1, phycoerythrin [PE]), CD4 (53-6.7, FITC), B220 (RA-6B2, biotin), IgM (eB121-15F9, FITC), IgD (11-26, PE), NK1.1 (PK136, biotin), and rat IgG2a monoclonal antibody (MAb) isotype control (eBR2a, pure) were from eBiosciences (San Diego, CA). CD3ε (145-2C11, PE), CD4 (PE), CD19 (PE), F4/80 (biotin), GR-1 (PE), and streptavidin (allophycocyanin) were purchased from Caltag (Towcester, United Kingdom). CD5 (53-7.3, biotin) and CD21 (7E9, FITC) were from BD PharMingen (San Diego, CA), CD23 (2G8, PE) was from Southern Biotechnology (Birmingham, AL), CCR3 (PE) was from R&D Systems (Minneapolis, MN), and MAb anti-rat IgG2a (FITC) was from Serotec (Kidlington, Oxford, United Kingdom). FITC-conjugated streptavidin was purchased from Vector Laboratories (Peterborough, United Kingdom). Affinity-purified polyclonal sheep anti-Siglec-E (FITC) and Siglec-F (Alexa 448 or biotin) were prepared and labeled in our own lab (48). CR-Fc fusion protein and FA/11 anti-mouse CD68 were kind gifts from Luisa Martinez-Pomares (Sir William Dunn School of Pathology, Oxford, United Kingdom). Rat anti-Sn MAbs 1C2 and SER-4 (both IgG2a) were used as tissue supernatant (9) and rabbit anti-Sn serum was used as an affinity-purified antibody (11).

Generation of Sn-deficient mice. Sn-deficient mice were generated by targeting the *Sn* gene in embryonic stem (ES) cells by homologous recombination (Fig. 1A). The Sn homology region was subcloned from a phage library (EMBL3) of 129/Sv mouse genomic DNA (31) kindly provided by Anna Marie-Frishauf, CRUK, London, United Kingdom. A 4.9-kb EcoRI fragment was cloned into the multiple cloning site of vector pTZ18U (Bio-Rad, Herts, United Kingdom). The *Sn* gene was disrupted by insertion of a neomycin resistance gene expression cassette (neomycin cassette, derived from pMC1neopA; Stratagene, Cambridge, United Kingdom) into the unique XhoI site in exon III (Fig. 1A). For negative selection, a SalI/XhoI diphtheria toxin A expression cassette fragment was cloned from pSP72-TKPro-DTA-polyA (kindly supplied by F. Otto, ICRF, London, United Kingdom) into the SalI site within the multiple cloning site 5′ of the homology region. Constructs were linearized with SalI prior to transfection into R1 mouse ES cells at CRUK Clare Hall Laboratories. G418-resistant clones were screened for homologous recombination by Southern blotting using an XbaI-EcoRI probe (Fig. 1A). Multiple vector integrations were excluded by Southern blotting using the neomycin cassette as a probe. Two independently obtained ES clones that had undergone homologous recombination were used for blastocyst injection, and the resulting chimeric mice were bred to C57BL/6 mice. All mice used for the phenotype analysis were intercross offspring of heterozygotes backcrossed for eight generations onto a C57BL/6 background unless stated otherwise; age- and sex-matched mice at 8 to 12 weeks of age were used in all experiments. Genotyping of mice was performed by PCR using the following primers: for, CACCACGGTCACTGTGACAA, and rev, GGCCAT ATGTAGGGTCGTCT (MWG, Milton Keynes, United Kingdom). This resulted in a 468-bp product for the wild-type allele and a 1,729-bp product for the mutated allele (Fig. 1B). Mice were bred and maintained under specific-pathogen-free conditions. Animal experimentation was approved by the University of Dundee Animal Ethics Committee and was done under United Kingdom Home Office Project License PPL60/3187.

Real-time PCR. Total RNA from wild-type and Sn-deficient mouse spleens was purified using the RNeasy mini kit (QIAGEN Ltd., West Sussex, United Kingdom) and reverse transcribed using oligo$(dT)_{18}$ primer and the RevertAid first-strand cDNA synthesis kit (MBI Fermentas, St. Leon-Rot, Germany). Sn cDNA was quantified with an ABI PRISM 7000 sequence detection system using primers and probes specific to Sn from Applied Biosystems (Assays-on-Demand,

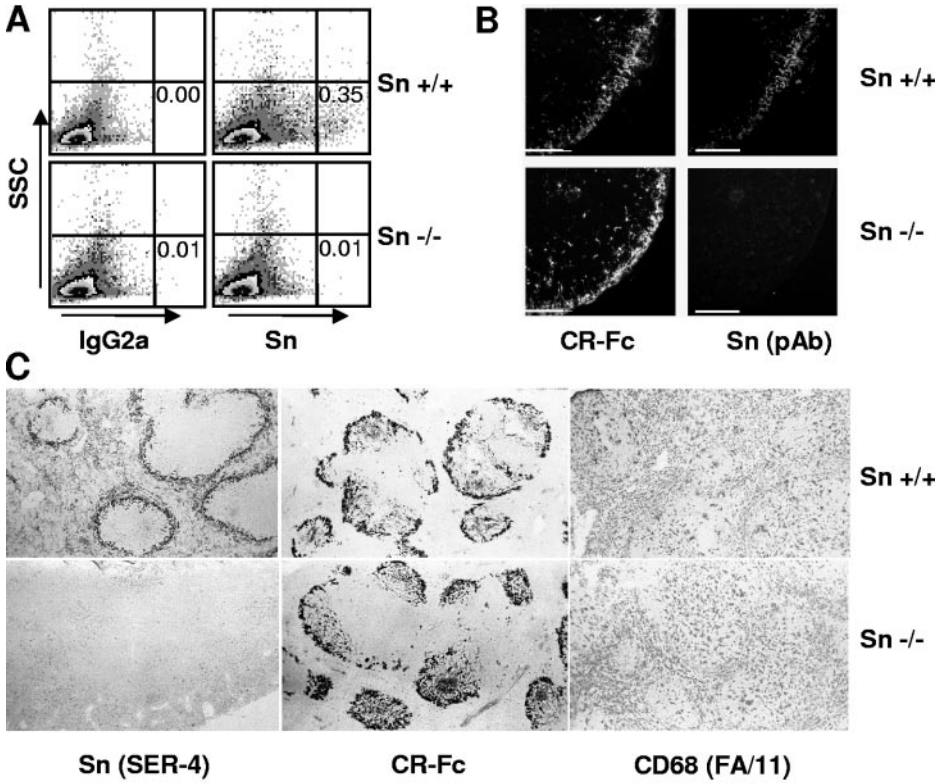

FIG. 2. Homozygous mutant mice lack detectable Sn expression. (A) FACS plots of single-cell suspensions of mesenteric lymph nodes stained for Sn surface expression using a mixture of anti-Sn MAb IC2 and SER-4. Dot plots show isotype control (IgG2a) and anti-Sn stainings plotted against the sideward scatter (SSC) for wild-type mice (top panels) and Sn-deficient mice (bottom panels). Percentages of positive cells are given within the quadrants. (B) Immunofluorescence staining of inguinal lymph node sections, double labeled with CR-Fc (left panels) and polyclonal antibody (PAb) anti-Sn (right panels), from wild-type and Sn-deficient mice. Shown are representative pictures of at least three independent experiments. The white bar indicates 100 μm. (C) Immunohistochemical analysis of spleen tissue sections from Sn wild-type (top panels) and Sn-deficient (bottom panels) mice that were stained with SER-4, CR-Fc, or anti-CD68 (FA/11). Representative pictures from several independent experiments are shown.

Foster City, CA). Sn primers span exon X to exon XI. Sn mRNA expression was normalized to the mRNA of TATA box binding protein. $\Delta\Delta C_T$ values were calculated after confirming similar amplification efficiencies of target and endogenous control cDNA.

Immunohistochemistry and immunofluorescence. Spleens and inguinal lymph nodes were embedded in OCT resin (Agar Scientific, Essex, United Kingdom) and frozen in a 2-methylbutane/dry ice bath. Cryostat sections (7 μm) were fixed for 10 min in acetone. For immunofluorescence, slides were blocked with 4% sheep serum in phosphate-buffered saline (PBS) and stained with polyclonal antibody anti-Sn (1 μg/ml) and CR-Fc (5 μg/ml) in 0.25% bovine serum albumin (BSA)/PBS, followed by the secondary antibodies goat anti-human IgG Fc-FITC (1:60) and goat anti-rabbit IgG-tetramethyl rhodamine isocyanate (1:30) for 1 h in a humidified container. Sections were mounted with 20% wt/vol Mowiol 4-88 (Calbiochem) and 20% vol/vol glycerol in PBS and analyzed using an Axioskop microscope (Zeiss, Munich, Germany) and Axio Vision 3.0 software. Immunoperoxidase staining of tissue sections was carried out using the avidin-biotin-peroxidase staining system (Vectastain; Vector Laboratories, Peterborough, United Kingdom) as described previously (9).

Flow cytometry. Single-cell suspensions were prepared from spleen, femoral bone marrow, lymph nodes, peritoneal cavity, and blood collected from mice euthanized with CO_2. In some experiments, spleen and lymph nodes were digested with 0.1% collagenase A (Roche, East Sussex, United Kingdom) and 0.01% DNase (Roche) in RPMI 1640 with 5% fetal calf serum for 30 min at 37°C. Cells were separated by passing them through a cell strainer and washed in PBS-EDTA (5 mM). Prior to staining, blood, splenocytes, and bone marrow cells were subjected to red blood cell lysis (RBL buffer; Sigma). Cells were routinely incubated with 2.4G2 MAb to block Fc receptors and subsequently labeled with antibodies diluted in PBA (PBS, 1% BSA, 0.05% azide) for 20 min on ice. In some cases, a secondary incubation step using an FITC-labeled secondary antibody or allophycocyanin- or FITC-conjugated streptavidin was added. Cells were finally stained with 7-amino actinomycin D to exclude dead cells and analyzed using a FACSCalibur (Becton Dickinson, Oxford, United Kingdom) and CellQuest software.

Thioglycolate-induced inflammation. Mice were injected intraperitoneally with 0.5 ml 3.8% Brewer modified thioglycolate medium (Becton Dickinson). After 4 h or 18 h, animals were euthanized by CO_2 inhalation and cells were collected by peritoneal lavage using 5 ml of cold PBS.

Isotype specific ELISA. Antibody titers were determined by enzyme-linked immunosorbent assay (ELISA) using Immulon 4 HBX plates (Thermo Labsystems) coated with goat anti-mouse immunoglobulin (5 μg/ml; Southern Biotechnology, Birmingham, AL) diluted in carbonate buffer. A standard curve was generated with purified mouse IgM, IgG1, IgG2a, IgG2b, and IgG3 (Southern Biotechnology). Plates were blocked with 1% BSA-0.2% gelatin in PBS for 1 h at room temperature, and sera were diluted in blocking buffer (IgM and IgG1, 1:5,000; IgG2a and IgG3, 1:10,000; and IgG2a, 1:25;000) and allowed to bind to the plate for 1 h at room temperature. Antibodies were detected by alkaline phosphatase-coupled immunoglobulin isotype-specific antibodies (Southern Biotechnology) and the substrate fluorescein diphosphate (Molecular Probes, Paisley, United Kingdom). Optical densities at 530 nm were measured with a fluorescent plate reader (Cytofluor; PerSeptive Biosystems).

RESULTS

Generation of Sn-deficient mice. To study the biological functions of Sn, we generated Sn-deficient mice through conventional gene targeting in ES cells in which the neomycin

TABLE 1. FACS analysis of cell populations in untreated wild-type control and Sn-deficient mice

Substance location[a]	Cell populations[b]	% of cells[c]	
		$Sn^{+/+}$	$Sn^{-/-}$
Bone marrow (n = 12–15)	T cells (CD3)	3.0 ± 1.0	2.7 ± 0.6
	B cells (CD19)	15.7 ± 3.2	18.4 ± 3.6
	Prepro B cells ($B220^h$ IgM^{low})	11.8 ± 2.0	12.6 ± 2.9
	Immature B cells ($B220^h$ IgM^{mid})	3.6 ± 0.5	3.4 ± 0.8
	Transitional B cells ($B220^h$ IgM^h)	2.7 ± 0.6	3.3 ± 0.8
	Mature B cells ($B220^{bright}$ IgM^{mid})	5.4 ± 0.7	5.7 ± 1.1
	NK cells (NK 1.1)	1.2 ± 0.8	1.3 ± 0.3
	Neutrophils (GR-1^+, Siglec E^+)	35.8 ± 5.5	32.5 ± 5.0
	Eosinophils ($CCR3^+$, Siglec F^+)	1.4 ± 0.5	1.4 ± 0.5
Blood (n = 13–15)	T cells (CD3)	22.6 ± 4.6	23.8 ± 7.0
	B cells (CD19)	43.8 ± 8.2	41.0 ± 10.8
	NK cells (NK 1.1)	5.3 ± 1.4	5.9 ± 2.2
	Neutrophils (GR-I^+ Siglec E^+)	14.9 ± 7.9	12.0 ± 6.8
	Eosinophils ($CCR3^+$ Siglec F^+)	1.9 ± 0.8	1.9 ± 0.8
Peritoneum (n = 13–15)	T cells (CD3)	10.4 ± 2.9	9.9 ± 2.8
	B cells (CD19)	57.4 ± 7.0	58.7 ± 5.5
	NK cells (NK 1.1)	0.8 ± 0.2	1.0 ± 0.2
	Macrophages (GR-1^{low} $F4/80^+$)	22.9 ± 3.7	26.4 ± 7.1
	Eosinophils ($CCR3^+$ Siglec F^+)	0.6 ± 0.4	0.6 ± 0.2
Spleen (n = 12)	T cells (CD3)	28.8 ± 2.8	31.6 ± 4.0
	$CD4^+$	21.6 ± 1.3	21.0 ± 3.3
	$CD8^+$	8.2 ± 0.9	12.2 ± 2.0***[e]
	B cells (B220)	61.0 ± 2.5	55.6 ± 3.3***
	T1 B cells (IgM^h IgD^{low})[d]	12.2 ± 1.0	14.4 ± 2.2**
	T2 B cells (IgM^h IgD^h)[d]	12.4 ± 2.0	13.8 ± 2.9
	Mature B cells (IgM^{low} IgD^h)[d]	64.2 ± 2.2	61.9 ± 4.8
	NK cells (NK 1.1)	2.2 ± 0.5	2.9 ± 0.4**
Lymph node (n = 8)	T cells (CD3)	54.0 ± 4.4	58.9 ± 3.4*
	$CD4^+$	37.3 ± 2.3	34.5 ± 2.7
	$CD8^+$	16.9 ± 1.5	23.9 ± 2.3***
	B cells (B220)	42.1 ± 4.3	37.1 ± 3.3*
	T1 B cells (IgM^h IgD^{low})[d]	6.9 ± 1.0	5.2 ± 1.1**
	T2 B cells (IgM^h IgD^h)[d]	23.9 ± 4.5	29.6 ± 3.8*
	Mature B cells (IgM^{low} IgD^h)[d]	59.6 ± 4.2	55.6 ± 3.5
	NK cells (NK 1.1)	0.6 ± 0.1	0.6 ± 0.1

[a] Total numbers of leukocytes recovered were $1.4 \times 10^7 \pm 4.4 \times 10^6$ and $1.6 \times 10^7 \pm 4.7 \times 10^6$ from bone marrow (one femur), $2.4 \times 10^6 \pm 1.0 \times 10^6$ and $2.6 \times 10^6 \pm 1.0 \times 10^6$ from peritoneal cavity, $9.6 \times 10^7 \pm 2.4 \times 10^7$ and $1.0 \times 10^8 \pm 2.9 \times 10^7$ from spleen, and $2.4 \times 10^7 \pm 9.3 \times 10^6$ and $2.3 \times 10^7 \pm 8.0 \times 10^6$ from mesenteric lymph nodes for $Sn^{+/+}$ and $Sn^{-/-}$ mice, respectively.

[b] h, high levels of expression.

[c] Data are given as the mean % of total cells ± SD from two to three independent experiments, except where indicated otherwise.

[d] Data are given as the mean % of $B220^+$ cells ± SD from two to three independent experiments.

[e] Asterisks indicate the degree of significance applying the t test: *, $P < 0.05$; **, $P < 0.01$; ***, $P < 0.001$.

cassette was inserted into exon III encoding the second immunoglobulin-like domain of Sn (31). Homologous recombination was identified in Southern blots by generation of a novel 5.9-kb XbaI fragment relative to a 4.7-kb endogenous fragment when probed with an upstream genomic XbaI-EcoRI probe (data not shown). Of 250 G418-resistant ES clones examined, three clones carried the neomycin cassette insertion. Two of the clones were selected for blastocyst injection, and both resulted in germ line transmission. Mice that were homozygous for the mutation were obtained from heterozygous intercrosses which gave rise to the expected Mendelian ratios of wild-type, heterozygous mutant, and homozygous mutant progeny. Under specific-pathogen-free conditions, the Sn-deficient mice showed no developmental abnormalities, and their growth was equivalent to that of their wild-type littermates (data not shown). Analysis by quantitative real-time PCR revealed that Sn mRNA in spleen is still produced at low levels despite the neomycin cassette insertion (Fig. 1C).

Sn expression. Sn is expressed at its highest levels on the subcapsular sinus macrophages in lymph nodes and on marginal metallophilic macrophages in spleen. In order to verify the absence of Sn protein in Sn-deficient mice, we performed fluorescence-activated cell sorter (FACS) analysis for mesenteric lymph node single-cell suspensions. Using a mixture of two monoclonal antibodies specific for Sn, IC2 and SER-4 directed to domains 1 and 3, respectively, about 0.35% of cells isolated from lymph nodes of wild-type mice were strongly labeled. In contrast, no staining above the isotype control background was observed in single-cell suspensions from Sn-deficient lymph nodes (Fig. 2A). We also analyzed tissue sections from lymph nodes by immunofluorescence and immunoperoxidase labeling. Staining of mesenteric lymph nodes using a

TABLE 2. FACS analysis of cell populations in wild-type control and Sn-deficient mice 18 h after intraperitoneal injection of thioglycolate broth

Substance location[a]	Cell populations	% of total cells[b]	
		$Sn^{+/+}$	$Sn^{-/-}$
Bone marrow (n = 13–15)	T cells (CD3)	2.6 ± 0.8	3.1 ± 1.0
	B cells (CD19)	17.6 ± 2.5	22.0 ± 4.2**[c]
	Neutrophils (GR-I^+ Siglec E^+)	25.5 ± 5.1	25.4 ± 5.9
	Eosinophils ($CCR3^+$ Siglec F^+)	1.0 ± 0.7	0.8 ± 0.3
Blood (n = 13–15)	T cells (CD3)	23.1 ± 4.3	22.0 ± 3.4
	B cells (CD19)	48.9 ± 3.8	44.6 ± 9.6
	NK cells (NK 1.1)	8.3 ± 2.0	9.3 ± 2.9
	Neutrophils (GR-I^+ Siglec E^+)	7.3 ± 3.2	8.0 ± 3.5
	Eosinophils ($CCR3^+$ Siglec F^+)	0.3 ± 0.2	0.4 ± 0.2
Peritoneum (n = 13–15)	T cells (CD3)	3.3 ± 1.0	3.8 ± 2.1
	B cells (CD19)	15.1 ± 4.3	14.0 ± 5.8
	NK cells (NK 1.1)	16.5 ± 5.1	16.3 ± 3.2
	Neutrophils (GR-I^+ Siglec E^+)	22.7 ± 7.7	29.8 ± 8.7*
	Monocytes (GR-I^+ $F4/80^+$)	17.5 ± 3.4	18.6 ± 6.8
	Eosinophils ($CCR3^+$ Siglec F^+)	24.9 ± 4.1	18.8 ± 5.3**

[a] Total numbers of leukocytes recovered were $2.1 \times 10^7 \pm 5.3 \times 10^6$ and $1.8 \times 10^7 \pm 8.2 \times 10^6$ from bone marrow and $1.6 \times 10^7 \pm 3.8 \times 10^6$ and $1.6 \times 10^7 \pm 5.1 \times 10^6$ from peritoneal cavity for $Sn^{+/+}$ and $Sn^{-/-}$ mice, respectively.
[b] Data are given as the mean percentage of total cells ± SD from three independent experiments.
[c] Asterisks indicate the degree of significance applying the t test: *, $P < 0.05$; **, $P < 0.01$; ***, $P < 0.001$.

polyclonal rabbit anti-Sn serum demonstrated that Sn is expressed within only the subcapsular sinus from wild-type but not Sn-deficient mice. To see if subcapsular macrophages were still present in Sn-deficient mice, staining was performed using the CR-Fc fusion protein shown previously to colocalize with this macrophage subset (26). No obvious differences were seen when wild-type and Sn-deficient mice were compared (Fig. 2B). Similar findings were made in the spleen using a highly sensitive avidin-biotin peroxidase staining method (Fig. 2C). The spleen sections of wild-type mice showed typical intense staining of marginal metallophilic macrophages at the inner regions of the marginal zones using the SER-4 MAb and a somewhat weaker staining of macrophages in the red pulp (Fig. 2C, top left). No Sn staining was detectable in spleen sections from Sn-deficient mice (Fig. 2C, bottom left), but the metallophilic macrophages were present normally as shown by staining with the CR-Fc protein (Fig. 2C, middle). The general distribution of macrophages was also normal, as revealed by staining with the panmacrophage marker CD68 (Fig. 2C, right). Finally, spleen sections were also stained with an affinity-purified rabbit antibody directed to a peptide from the C-terminal cytoplasmic tail of Sn. This gave staining similar to that of SER-4 in wild-type mice but no detectable staining of sections from Sn-deficient mice (data not shown). Taken together, these findings establish unequivocally that the $Sn^{-/-}$ mice are true nulls and that the lack of sialoadhesin does not lead to obvious changes either in localization and numbers of lymphoid and splenic macrophage populations or in the overall tissue architecture.

Sn deficiency does not affect the cellular composition of bone marrow. Sn has been found previously to bind strongly to granulocytes (8) and to be clustered in contact zones of Sn-positive macrophages and developing granulocytes in bone marrow (13). We therefore hypothesized that Sn may play a role in the development of granulocytes or in their retention within the bone marrow. Analyzing the bone marrow for immature and mature granulocytes using antibodies to a range of markers, including GR-1, NK1.1, mSiglec-E, mSiglec-F, and CCR3, we found no differences in cellular composition between wild-type and Sn-deficient mice (Table 1). In order to see whether Sn influences the cell pools in other compartments by retaining granulocytes in the bone marrow, we extended the analysis to blood and peritoneal cavity lavages, but again we could not detect any differences in cell percentages (Table 1). Also, the percentages of total T cells and B cells did not change in all three tissues (Table 1).

Sn deficiency does not significantly affect thioglycolate-induced inflammation in the peritoneal cavity. As shown above, there were no differences in neutrophil and eosinophil numbers in bone marrow and blood between Sn-deficient and wild-type mice under steady-state conditions. We next asked whether myeloid cells would be recruited more readily after an inflammatory stimulus in the Sn-deficient mice. At 4 h after intraperitoneal injection of thioglycolate into wild-type and Sn-deficient mice, there was a slight reduction in numbers of newly recruited neutrophils in Sn-deficient mice, but this difference was not statistically significant (percent cells for $Sn^{+/+}$, 42.5 ± 7.6; percent cells for $Sn^{-/-}$, 36.4 ± 6.9). At 18 h after injection, a small increase in neutrophil numbers was observed in Sn-deficient mice, and this was accompanied by a modest decrease in eosinophils compared to that for wild-type mice (Table 2). No differences were seen in numbers of monocytes recruited to the peritoneal cavity. In addition, no differences were noticed in blood and only a small increase in percentages of B cells in bone marrow from Sn-deficient mice was noted (Table 2). In conclusion, the absence of Sn from resident bone marrow macrophages does not have a significant effect on myeloid cell development or recruitment of myeloid cells during acute inflammatory responses.

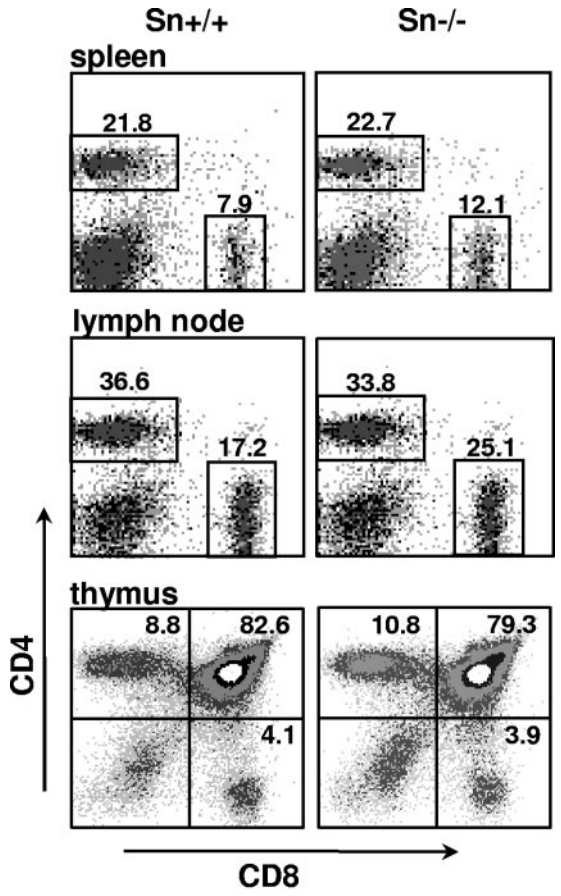

FIG. 3. Sn-deficient mice show an increase in CD8 T cells in the periphery but normal T-cell development. Single-cell suspensions from spleen, lymph node, or thymus were stained with antibodies directed to CD4 and CD8 and analyzed by FACS. Representative density plots of at least two independent experiments (n = 6 to 12) from mice aged 12 to 13 weeks are shown. Spleen and lymph node results are also summarized in Table 1. Percentages of cells within the gates for each sample are given.

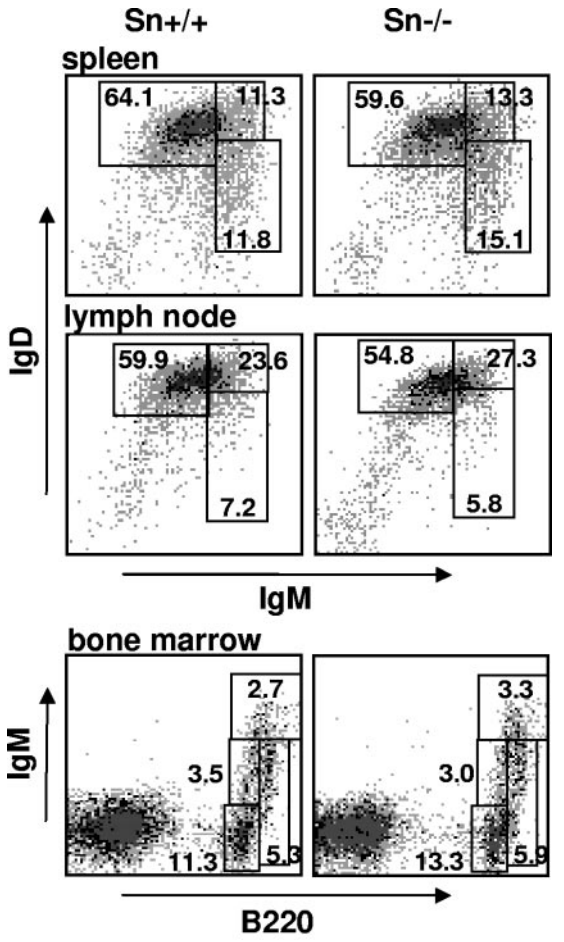

FIG. 4. Sn-deficient mice show unaltered B-cell maturation. Single-cell suspensions from spleen, lymph node, or bone marrow were stained with antibodies directed to B220 and IgM and IgD. Representative density plots of B220-positive cells (spleen and lymph node) or total cells (bone marrow) of at least two independent experiments (n = 8 to 12) are shown. Gates shown in the plot from bone marrow cells represent, starting from the bottom left clockwise, prepro-, immature, transient, and mature B cells. Results are also summarized in Table 1. Percentages of cells within the gates for each sample are given.

Subtle changes in T- and B-cell population in Sn-deficient mice. Sn is strongly expressed by marginal metallophilic macrophages in spleen and subcapsular sinus macrophages in lymph nodes. When splenocytes were analyzed by FACS, a small but very consistent increase in the percentage of CD8 T cells in Sn-deficient mice was observed (8.2 ± 0.9 to 12.2 ± 2.0), while CD4 T cells remained unchanged (Table 1 and Fig. 3). This resulted in a change of the CD4/CD8 T-cell ratio from 2.7 ± 0.2 in wild-type to 1.8 ± 0.4 in Sn-deficient mice. A very similar decrease in the CD4/CD8 T-cell ratio from 2.2 ± 0.2 to 1.5 ± 0.2 in Sn-deficient mice was seen in mesenteric lymph nodes (Table 1 and Fig. 3). Although Sn is only weakly expressed on macrophages in the thymus, we analyzed thymocytes in order to see whether T-cell development is affected. However, we failed to find any difference in percentage of CD4 single-positive ($Sn^{+/+}$ 10.6 ± 1.8 and $Sn^{-/-}$ 11.3 ± 0.9), CD8 single-positive ($Sn^{+/+}$ 4.1 ± 0.5 and $Sn^{-/-}$ 3.6 ± 0.4) or double-positive thymocytes ($Sn^{+/+}$ 80.7 ± 2.8 and $Sn^{-/-}$ 80.1 ± 1.4) from either 12-week-old (Fig. 3) or 5-week-old mice (data not shown).

To compare B-cell subsets in spleen, we performed triple staining for IgM, IgD, and B220 expression and observed a small but very consistent decrease in B220-positive cells in Sn-deficient mice (Table 1). In comparison, the pattern of IgM and IgD expression, indicating the maturation status of B lymphocytes (14, 34), was unaltered (Fig. 4). A similar decrease in B220-positive cells was seen in lymph nodes from Sn-deficient mice, again with no change in maturation status of B cells (Table 1; Fig. 4). B-cell maturation in bone marrow was also unaffected by Sn deficiency, as determined by IgM and B220 double staining, defining prepro-, immature, transient, and mature B cells (15, 22) (Table 1; Fig. 4). In summary, CD8 T cells were increased in Sn-deficient mice and this was accompanied by a decrease in B220-positive cells in both spleen and lymph node.

Reduced IgM levels in Sn-deficient mice. In view of the decrease of B220-positive cells in Sn-deficient mice, we next analyzed levels of serum immunoglobulin classes. Interestingly,

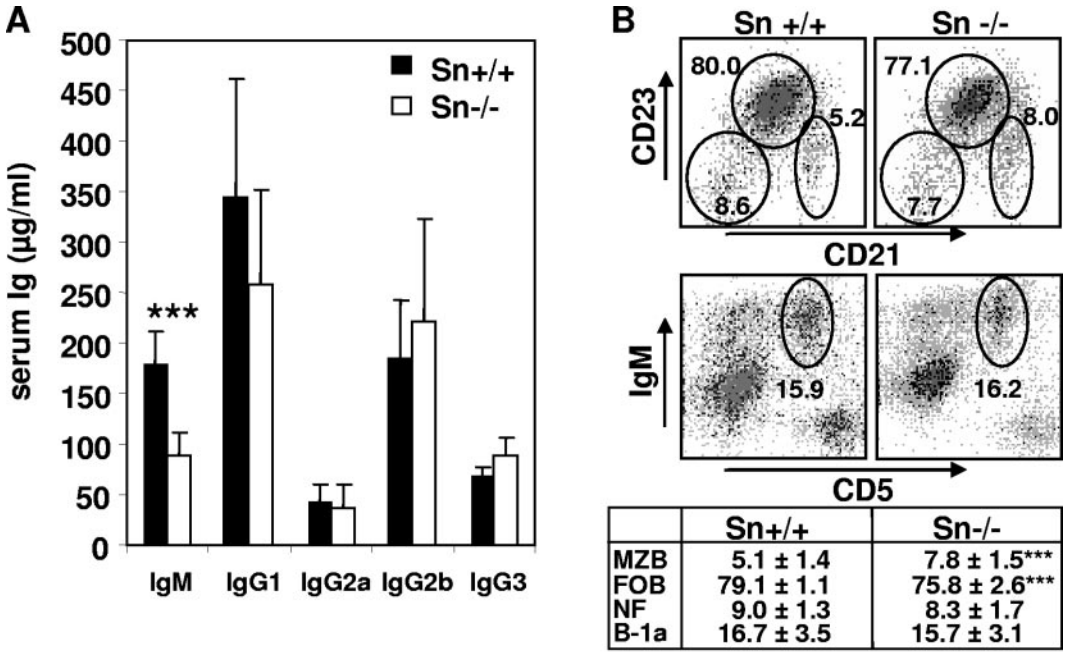

	Sn+/+	Sn-/-
MZB	5.1 ± 1.4	7.8 ± 1.5***
FOB	79.1 ± 1.1	75.8 ± 2.6***
NF	9.0 ± 1.3	8.3 ± 1.7
B-1a	16.7 ± 3.5	15.7 ± 3.1

FIG. 5. Sn-deficient mice show decreased IgM serum levels but no decrease in natural antibody-producing cells. (A) Total serum immunoglobulins from age-matched 3- to 6-month-old mice measured by ELISA ($n = 10$). Asterisks indicate that the degree of significance from applying the t test was P of <0.001. (B) Single-cell suspensions from spleen (top panels) or from peritoneal lavage fluid (bottom panels) were analyzed for B-cell subsets by flow cytometry. Representative density plots of B220-positive cells (for spleen, newly formed [NF] $CD21^-$ $CD23^-$; follicular B [FOB], $CD21^{+/-}$ $CD23^+$; and MZB, $CD21^+CD23^-$) or total cells (for bone marrow, B-1a, IgM^+ $CD5^+$) are shown. Below data are summarized as mean percentage of $B220^+$ (MZB, FOB, and NF) or total cells (B-1a) ± SD from three independent experiments ($n = 12$). ***, $P < 0.001$.

Sn-deficient mice showed a reduction of more than 50% in serum IgM antibodies, which was statistically highly significant (Fig. 5A). There was a small but statistically nonsignificant decrease in IgG1 levels, and IgG2a, IgG2b, and IgG3 levels were unaltered. Since these mice were kept under specific-pathogen-free conditions, we suspected that the decrease in IgM levels could be due to a lack of natural antibodies, which constitute a large portion of serum IgM. The major source of natural antibodies are peritoneal $CD5^+$ B-1a cells and marginal zone B (MZB) cells, which lie in close proximity to Sn-positive marginal metallophilic macrophages (27, 36). We therefore compared wild-type and Sn-deficient mice for their content of marginal zone B cells ($CD23^-$ $CD21^+$) (15, 40) in spleen and B-1a cells ($B220^{low}$ $CD11b^+$ IgM^+ $CD3^-$ $CD5^+$) (47) in the peritoneal cavity. Within the B220-positive population, we found a decrease in the percentage of follicular B cells ($CD23^+$ $CD21^-$) in Sn-deficient mice and, surprisingly, an increase in the percentage of MZB cells ($CD23^-$ $CD21^+$) (Fig. 5B). The newly formed B cells ($CD23^-$ $CD21^-$) did not change. A similar increase in percentage was observed when defining the MZB cell population as $CD1d^{bright}$ $B220^+$ cells (40) (data not shown). No significant difference was detected for B-1a cells from peritoneal lavage fluid samples, defined here as IgM^+ $CD5^+$ cells (Fig. 5B) or $CD3^-$ $B220^-CD5^+$ (data not shown).

DISCUSSION

Sialoadhesin is a highly conserved molecule that is expressed on similar subsets of macrophages in all the mammalian species examined. Its molecular features suggest that it is likely to be involved in cell-cell or cell-matrix interactions. This initial characterization of Sn-deficient mice reveals that these mice show a very mild phenotype when housed under specific-pathogen-free conditions, and the overall results suggest that Sn is involved in regulation of the immune system rather than in steady-state hematopoiesis. The fact that Sn was previously found to bind selectively to neutrophils and to cluster in contact zones between macrophages and developing granulocytes but not erythroblasts in the bone marrow gave rise to the idea that Sn may be involved in the development of granulocytes or may regulate their release into the circulation. However, analysis of neutrophil and eosinophil numbers in resting as well as in thioglycolate-stimulated Sn-deficient mice did not reveal gross alterations from wild-type mice. We conclude from this that the major role of Sn is not in the regulation of granulocyte production or release from the marrow under steady-state or acute inflammatory conditions.

More detailed analysis of cell populations revealed that Sn-deficient mice have relatively more CD8 T cells in spleen and lymph node compared to wild-type mice, while the CD4 T-cell population is unaltered. Since no changes were found in T-cell development in the thymus, Sn most likely has an impact on T-cell homeostasis in the periphery. It remains to be seen whether these additional CD8 T cells have an altered phenotype and whether the increase is due to altered recirculation, increased proliferation, or decreased apoptosis. Although we used wild-type and Sn-deficient mice backcrossed for at least eight generations onto a C57BL/6 background, we cannot completely rule out the possibility that minor additional genetic

differences account for these small changes. However, sialylation of T cells has been shown to change dramatically during T-cell development and activation and to affect their potential as effector cells (28, 30, 43). Although resting lymphocytes interact only very weakly with Sn, there are indications that activated T cells do express Sn counterreceptors (8, 45). The enzyme most likely responsible for these changes is the sialyltransferase ST3GalI, which sialylates O-glycans on molecules like CD43, previously shown to be the counterreceptor for Sn on T cells (45). Interestingly, in ST3GalI-deficient mice, CD8 T-cell homeostasis is also altered, resulting in a profound loss of CD8 T cells in spleen, while the CD4 population and thymocytes are unaffected (29, 38). For these mice, it was shown that CD8 T cells undergo massive apoptosis in spleen. Whether there is a link between these directly opposing phenotypes remains to be seen, but both findings emphasize the importance of α2,3 sialylation for CD8 T-cell homeostasis. The selectivity for CD8 T cells could be due to the fact that α2,3-linked sialic acids on CD4 T cells are heavily 9-O acetylated (24), a modification that prevents recognition by Sn (19). It remains to be shown whether the increase in CD8-positive T cells has a functional consequence in Sn-deficient mice.

We also found a small decrease in B220-positive cells in spleen and lymph nodes from Sn-deficient mice which may be a compensatory effect of the increase in CD8 T cells. In spleen, this appeared to correspond to a reduction in follicular B cells. However, the maturation of B cells in bone marrow, lymph nodes, and spleen seemed to be unaltered. Sn in spleen is very strongly expressed on marginal metallophilic macrophages. These cells occupy a prime position on the inner side of the marginal zone, where lymphocytes, blood-borne antigen, and antigen-presenting cells enter the white pulp. They are also in close proximity to B-cell follicles and the marginal zone B cells. We found that soluble IgM levels were reduced by about 50% in Sn-deficient mice, while IgG levels were unaltered. A reasonable hypothesis was that this is due to reduced levels of natural antibodies, but we did not find any indication that natural antibody-producing cells were reduced in number. B-1a cell numbers in the peritoneal cavity were normal, and marginal zone B cells were even slightly increased. Furthermore, there was no alteration in the percentage of cells staining positive for membrane IgM or its staining intensity using FACS analysis.

Interestingly, mice deficient in secreted IgM exhibit rather normal B-cell development and serum IgG levels (3), but this is accompanied by a pronounced increase in natural antibody-producing cells. These mice have a T-dependent IgG response that is impaired with only suboptimal, not optimal, doses of antigen. It remains to be seen whether this is also true for Sn-deficient mice. Experiments with secreted IgM-deficient mice have also demonstrated a critical role of natural IgM in the immediate defense against systemic bacterial infection (4). It will be interesting to see whether Sn-deficient mice are more susceptible to microbial infections in general. It will also be important to examine the susceptibility of Sn-deficient mice to sialylated and nonsialylated pathogens in order to investigate its role in sialic acid-dependent clearance functions. How Sn deficiency results in reduced IgM titers in unchallenged mice is currently unclear. However, there is evidence that Sn-positive macrophages localize within primary B-cell follicles during the initial priming of antibody responses (2). Clearly, further investigation is needed to analyze the role of Sn in eliciting humoral immune responses and cell trafficking upon antigen challenge.

The fact that Sn is highly conserved within mammals relative to the rapidly evolving CD33-related Siglecs (1), together with its very distinct expression pattern, suggests that there are specific functions of Sn that are conserved between mammals. Since steady-state hematopoiesis appears unaffected in Sn-deficient mice, we speculate that the primary role of Sn may be in regulating the immune system. Since specific-pathogen-free Sn-deficient mice have only a subtle phenotype, this makes them an ideal model to investigate the role of Sn in modulating immune and inflammatory responses.

ACKNOWLEDGMENTS

This work was supported by a Wellcome Trust Senior Fellowship.

We thank Ian Rosewell and the transgenic team at Clare Hall (Cancer Research UK) for ES cell work and embryo manipulation.

REFERENCES

1. **Angata, T., E. H. Margulies, E. D. Green, and A. Varki.** 2004. Large-scale sequencing of the CD33-related Siglec gene cluster in five mammalian species reveals rapid evolution by multiple mechanisms. Proc. Natl. Acad. Sci. USA **101:**13251–13256.
2. **Berney, C., S. Herren, C. A. Power, S. Gordon, L. Martinez-Pomares, and M. H. Kosco-Vilbois.** 1999. A member of the dendritic cell family that enters B cell follicles and stimulates primary antibody responses identified by a mannose receptor fusion protein. J. Exp. Med. **190:**851–860.
3. **Boes, M., C. Esau, M. B. Fischer, T. Schmidt, M. Carroll, and J. Chen.** 1998. Enhanced B-1 cell development, but impaired IgG antibody responses in mice deficient in secreted IgM. J. Immunol. **160:**4776–4787.
4. **Boes, M., A. P. Prodeus, T. Schmidt, M. C. Carroll, and J. Chen.** 1998. A critical role of natural immunoglobulin M in immediate defense against systemic bacterial infection. J. Exp. Med. **188:**2381–2386.
5. **Boyce, N. W., S. R. Holdsworth, C. D. Dijkstra, and R. C. Atkins.** 1987. Quantitation of intraglomerular mononuclear phagocytes in experimental glomerulonephritis in the rat using specific monoclonal antibodies. Pathology **19:**290–293.
6. **Brinkman-Van der Linden, E. C., E. R. Sjoberg, L. R. Juneja, P. R. Crocker, N. Varki, and A. Varki.** 2000. Loss of *N*-glycolylneuraminic acid in human evolution. Implications for sialic acid recognition by siglecs. J. Biol. Chem. **275:**8633–8640.
7. **Crocker, P. R.** 2002. Siglecs: sialic-acid-binding immunoglobulin-like lectins in cell-cell interactions and signalling. Curr. Opin. Struct. Biol. **12:**609–615.
8. **Crocker, P. R., S. Freeman, S. Gordon, and S. Kelm.** 1995. Sialoadhesin binds preferentially to cells of the granulocytic lineage. J. Clin. Investig. **95:**635–643.
9. **Crocker, P. R., and S. Gordon.** 1989. Mouse macrophage hemagglutinin (sheep erythrocyte receptor) with specificity for sialylated glycoconjugates characterized by a monoclonal antibody. J. Exp. Med. **169:**1333–1346.
10. **Crocker, P. R., and S. Gordon.** 1986. Properties and distribution of a lectin-like hemagglutinin differentially expressed by murine stromal tissue macrophages. J. Exp. Med. **164:**1862–1875.
11. **Crocker, P. R., S. Mucklow, V. Bouckson, A. McWilliam, A. C. Willis, S. Gordon, G. Milon, S. Kelm, and P. Bradfield.** 1994. Sialoadhesin, a macrophage sialic acid binding receptor for haemopoietic cells with 17 immunoglobulin-like domains. EMBO J. **13:**4490–4503.
12. **Crocker, P. R., and A. Varki.** 2001. Siglecs in the immune system. Immunology **103:**137–145.
13. **Crocker, P. R., Z. Werb, S. Gordon, and D. F. Bainton.** 1990. Ultrastructural localization of a macrophage-restricted sialic acid binding hemagglutinin, SER, in macrophage-hematopoietic cell clusters. Blood **76:**1131–1138.
14. **Doody, G. M., S. E. Bell, E. Vigorito, E. Clayton, S. McAdam, R. Tooze, C. Fernandez, I. J. Lee, and M. Turner.** 2001. Signal transduction through Vav-2 participates in humoral immune responses and B cell maturation. Nat. Immunol. **2:**542–547.
15. **Girkontaite, I., K. Missy, V. Sakk, A. Harenberg, K. Tedford, T. Potzel, K. Pfeffer, and K. D. Fischer.** 2001. Lsc is required for marginal zone B cells, regulation of lymphocyte motility and immune responses. Nat. Immunol. **2:**855–862.
16. **Hartnell, A., J. Steel, H. Turley, M. Jones, D. G. Jackson, and P. R. Crocker.** 2001. Characterization of human sialoadhesin, a sialic acid binding receptor expressed by resident and inflammatory macrophage populations. Blood **97:**288–296.

17. **Jiang, H. R., L. Lumsden, and J. V. Forrester.** 1999. Macrophages and dendritic cells in IRBP-induced experimental autoimmune uveoretinitis in B10RIII mice. Investig. Ophthalmol. Vis. Sci. **40:**3177–3185.
18. **Jones, C., M. Virji, and P. R. Crocker.** 2003. Recognition of sialylated meningococcal lipopolysaccharide by siglecs expressed on myeloid cells leads to enhanced bacterial uptake. Mol. Microbiol. **49:**1213–1225.
19. **Kelm, S., R. Schauer, J. C. Manuguerra, H. J. Gross, and P. R. Crocker.** 1994. Modifications of cell surface sialic acids modulate cell adhesion mediated by sialoadhesin and CD22. Glycoconj. J. **11:**576–585.
20. **Kirchberger, S., O. Majdic, P. Steinberger, S. Bluml, K. Pfistershammer, G. Zlabinger, L. Deszcz, E. Kuechler, W. Knapp, and J. Stockl.** 2005. Human rhinoviruses inhibit the accessory function of dendritic cells by inducing sialoadhesin and B7-H1 expression. J. Immunol. **175:**1145–1152.
21. **Kumamoto, Y., N. Higashi, K. Denda-Nagai, M. Tsuiji, K. Sato, P. R. Crocker, and T. Irimura.** 2004. Identification of sialoadhesin as a dominant lymph node counter-receptor for mouse macrophage galactose-type C-type lectin 1. J. Biol. Chem. **279:**49274–49280.
22. **Lauzurica, P., D. Sancho, M. Torres, B. Albella, M. Marazuela, T. Merino, J. A. Bueren, A. C. Martinez, and F. Sanchez-Madrid.** 2000. Phenotypic and functional characteristics of hematopoietic cell lineages in CD69-deficient mice. Blood **95:**2312–2320.
23. **Liu, Y., A. J. Chirino, Z. Misulovin, C. Leteux, T. Feizi, M. C. Nussenzweig, and P. J. Bjorkman.** 2000. Crystal structure of the cysteine-rich domain of mannose receptor complexed with a sulfated carbohydrate ligand. J. Exp. Med. **191:**1105–1116.
24. **Martin, L. T., J. D. Marth, A. Varki, and N. M. Varki.** 2002. Genetically altered mice with different sialyltransferase deficiencies show tissue-specific alterations in sialylation and sialic acid 9-*O*-acetylation. J. Biol. Chem. **277:** 32930–32938.
25. **Martinez-Pomares, L., P. R. Crocker, R. Da Silva, N. Holmes, C. Colominas, P. Rudd, R. Dwek, and S. Gordon.** 1999. Cell-specific glycoforms of sialoadhesin and CD45 are counter-receptors for the cysteine-rich domain of the mannose receptor. J. Biol. Chem. **274:**35211–35218.
26. **Martinez-Pomares, L., M. Kosco-Vilbois, E. Darley, P. Tree, S. Herren, J. Y. Bonnefoy, and S. Gordon.** 1996. Fc chimeric protein containing the cysteine-rich domain of the murine mannose receptor binds to macrophages from splenic marginal zone and lymph node subcapsular sinus and to germinal centers. J. Exp. Med. **184:**1927–1937.
27. **McHeyzer-Williams, M. G.** 2003. B cells as effectors. Curr. Opin. Immunol. **15:**354–361.
28. **Merry, A. H., R. J. Gilbert, D. A. Shore, L. Royle, O. Miroshnychenko, M. Vuong, M. R. Wormald, D. J. Harvey, R. A. Dwek, B. J. Classon, P. M. Rudd, and S. J. Davis.** 2003. *O*-Glycan sialylation and the structure of the stalk-like region of the T cell co-receptor CD8. J. Biol. Chem. **278:**27119–27128.
29. **Moody, A. M., D. Chui, P. A. Reche, J. J. Priatel, J. D. Marth, and E. L. Reinherz.** 2001. Developmentally regulated glycosylation of the CD8αβ co-receptor stalk modulates ligand binding. Cell **107:**501–512.
30. **Moody, A. M., S. J. North, B. Reinhold, S. J. Van Dyken, M. E. Rogers, M. Panico, A. Dell, H. R. Morris, J. D. Marth, and E. L. Reinherz.** 2003. Sialic acid capping of CD8β core 1-*O*-glycans controls thymocyte-major histocompatibility complex class I interaction. J. Biol. Chem. **278:**7240–7246.
31. **Mucklow, S., S. Gordon, and P. R. Crocker.** 1997. Characterization of the mouse sialoadhesin gene, Sn. Mamm. Genome **8:**934–937.
32. **Muerkoster, S., M. Rocha, P. R. Crocker, V. Schirrmacher, and V. Umansky.** 1999. Sialoadhesin-positive host macrophages play an essential role in graft-versus-leukemia reactivity in mice. Blood **93:**4375–4386.
33. **Munday, J., H. Floyd, and P. R. Crocker.** 1999. Sialic acid binding receptors (siglecs) expressed by macrophages. J. Leukoc. Biol. **66:**705–711.
34. **Muto, A., S. Tashiro, O. Nakajima, H. Hoshino, S. Takahashi, E. Sakoda, D. Ikebe, M. Yamamoto, and K. Igarashi.** 2004. The transcriptional programme of antibody class switching involves the repressor Bach2. Nature **429:**566–571.
35. **Nath, D., A. Hartnell, L. Happerfield, D. W. Miles, J. Burchell, J. Taylor-Papadimitriou, and P. R. Crocker.** 1999. Macrophage-tumour cell interactions: identification of MUC1 on breast cancer cells as a potential counter-receptor for the macrophage-restricted receptor, sialoadhesin. Immunology **98:**213–219.
36. **Ochsenbein, A. F., and R. M. Zinkernagel.** 2000. Natural antibodies and complement link innate and acquired immunity. Immunol. Today **21:**624–630.
37. **Polman, C. H., C. D. Dijkstra, T. Sminia, and J. C. Koetsier.** 1986. Immunohistological analysis of macrophages in the central nervous system of Lewis rats with acute experimental allergic encephalomyelitis. J. Neuroimmunol. **11:**215–222.
38. **Priatel, J. J., D. Chui, N. Hiraoka, C. J. Simmons, K. B. Richardson, D. M. Page, M. Fukuda, N. M. Varki, and J. D. Marth.** 2000. The ST3Gal-I sialyltransferase controls $CD8^+$ T lymphocyte homeostasis by modulating *O*-glycan biosynthesis. Immunity **12:**273–283.
39. **Pulliam, L., B. Sun, and H. Rempel.** 2004. Invasive chronic inflammatory monocyte phenotype in subjects with high HIV-1 viral load. J. Neuroimmunol. **157:**93–98.
40. **Rolf, J., V. Motta, N. Duarte, M. Lundholm, E. Berntman, M. L. Bergman, L. Sorokin, S. L. Cardell, and D. Holmberg.** 2005. The enlarged population of marginal zone/CD1d(high) B lymphocytes in nonobese diabetic mice maps to diabetes susceptibility region Idd11. J. Immunol. **174:**4821–4827.
41. **Schadee-Eestermans, I. L., E. C. Hoefsmit, M. van de Ende, P. R. Crocker, T. K. van den Berg, and C. D. Dijkstra.** 2000. Ultrastructural localisation of sialoadhesin (siglec-1) on macrophages in rodent lymphoid tissues. Immunobiology. **202:**309–325.
42. **Shi, W. X., R. Chammas, N. M. Varki, L. Powell, and A. Varki.** 1996. Sialic acid 9-*O*-acetylation on murine erythroleukemia cells affects complement activation, binding to I-type lectins, and tissue homing. J. Biol. Chem. **271:** 31526–31532.
43. **Starr, T. K., M. A. Daniels, M. M. Lucido, S. C. Jameson, and K. A. Hogquist.** 2003. Thymocyte sensitivity and supramolecular activation cluster formation are developmentally regulated: a partial role for sialylation. J. Immunol. **171:**4512–4520.
44. **van den Berg, T. K., J. J. Breve, J. G. Damoiseaux, E. A. Dopp, S. Kelm, P. R. Crocker, C. D. Dijkstra, and G. Kraal.** 1992. Sialoadhesin on macrophages: its identification as a lymphocyte adhesion molecule. J. Exp. Med. **176:**647–655.
45. **van den Berg, T. K., D. Nath, H. J. Ziltener, D. Vestweber, M. Fukuda, I. van Die, and P. R. Crocker.** 2001. Cutting edge: CD43 functions as a T cell counterreceptor for the macrophage adhesion receptor sialoadhesin (Siglec-1). J. Immunol. **166:**3637–3640.
46. **Vanderheijden, N., P. L. Delputte, H. W. Favoreel, J. Vandekerckhove, J. Van Damme, P. A. van Woensel, and H. J. Nauwynck.** 2003. Involvement of sialoadhesin in entry of porcine reproductive and respiratory syndrome virus into porcine alveolar macrophages. J. Virol. **77:**8207–8215.
47. **Wilkinson, R., A. B. Lyons, D. Roberts, M. X. Wong, P. A. Bartley, and D. E. Jackson.** 2002. Platelet endothelial cell adhesion molecule-1 (PECAM-1/CD31) acts as a regulator of B-cell development, B-cell antigen receptor (BCR)-mediated activation, and autoimmune disease. Blood **100:**184–193.
48. **Zhang, J. Q., B. Biedermann, L. Nitschke, and P. R. Crocker.** 2004. The murine inhibitory receptor mSiglec-E is expressed broadly on cells of the innate immune system whereas mSiglec-F is restricted to eosinophils. Eur. J. Immunol. **34:**1175–1184.